Microporous Aluminophosphates Synthesized with 1,2,3-Trimethylimidazolium and Fluoride

Jeong Hwan Lee, Eun Jeong Kim, Fernando López-Arbeloa,
Suk Bong Hong and Miguel A. Camblor

Supporting Information

List of Figures

List of Tables

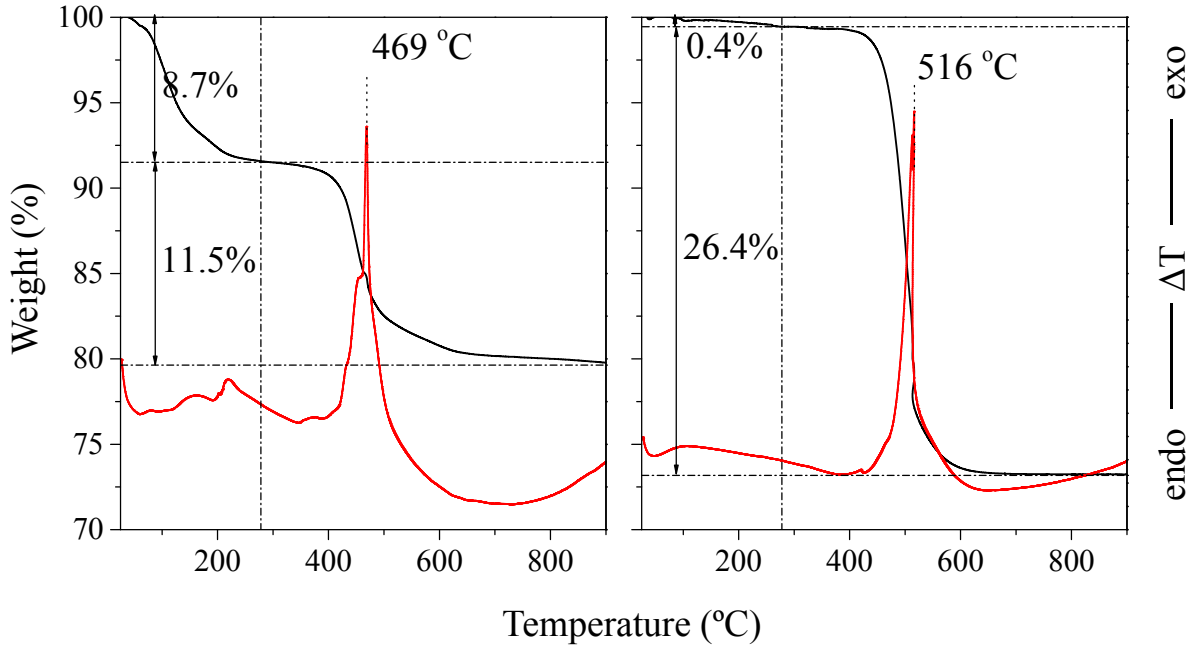

Figure S1: TGA/DTA (black/red) traces of as-made PST-27 (left) and triclinic $AlPO_4$–34 (right). The backwards shift of the TG trace of $AlPO_4$–34 around 550 ° C is due to the overheating caused by the combustion process associated to the main weight loss.

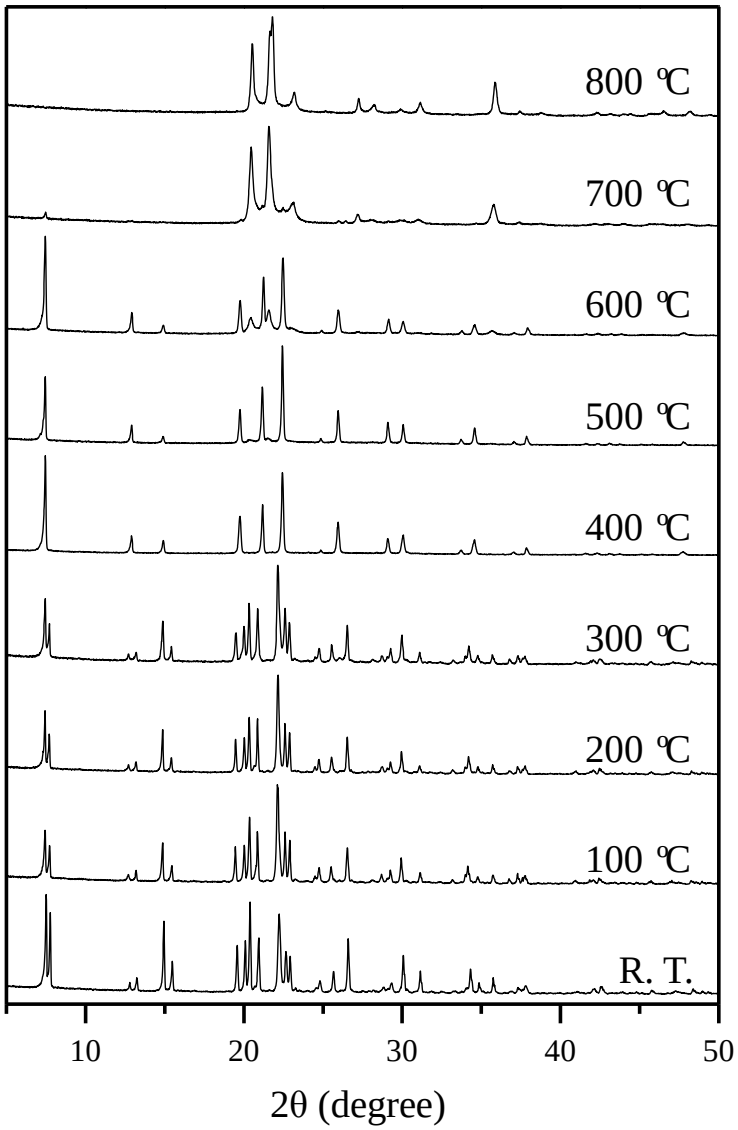

Figure S2: Ex-situ variable temperature XRD patterns of PST-27. The patterns were recorded at room temperature after calcination at the temperatures noted.

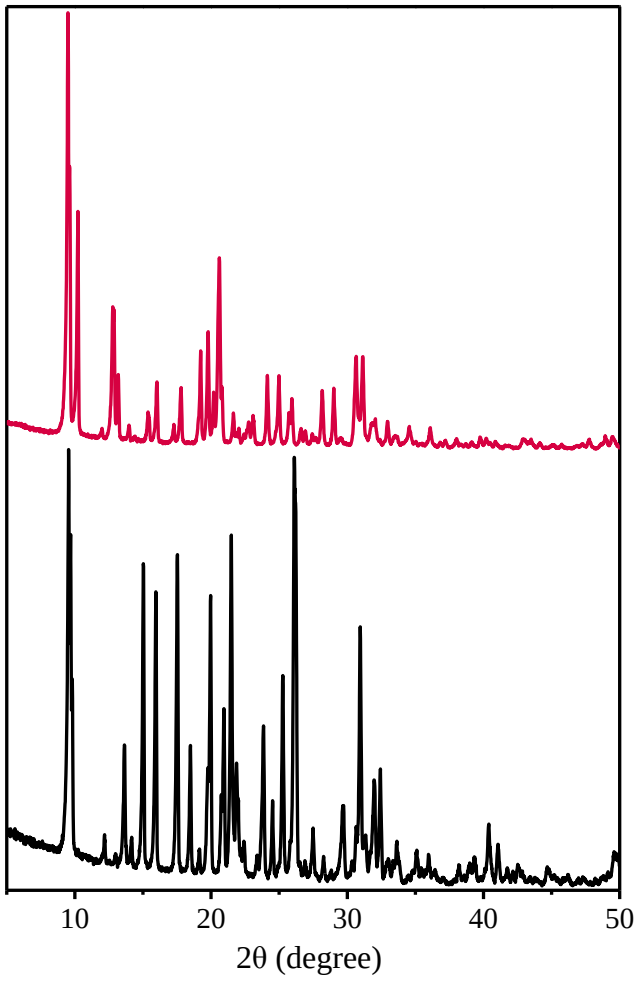

Figure S3: Powder XRD pattern (Cu K_α radiation) of as-made (bottom) and calcined (top, 550°C) triclinic 123TMIF–$AlPO_4$–34.

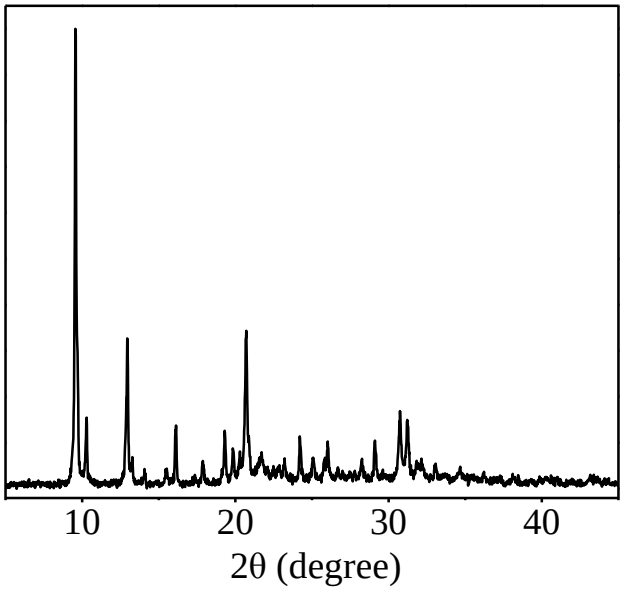

Figure S4: Powder XRD pattern (Cu K_α radiation) of triclinic 123TMIF–$AlPO_4$–34 after TGA/DTA analysis up to 1000 °C.

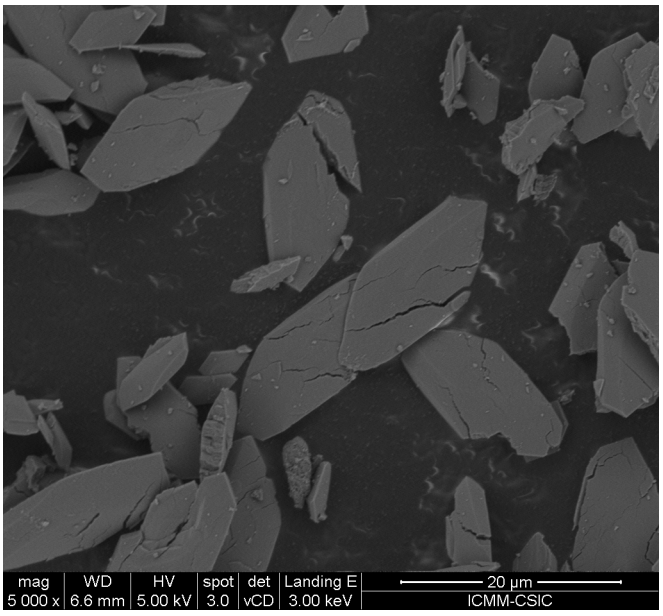

Figure S5: FESEM image of $AlPO_4$–34 after TGA/DTA analysis up to 1000 °C

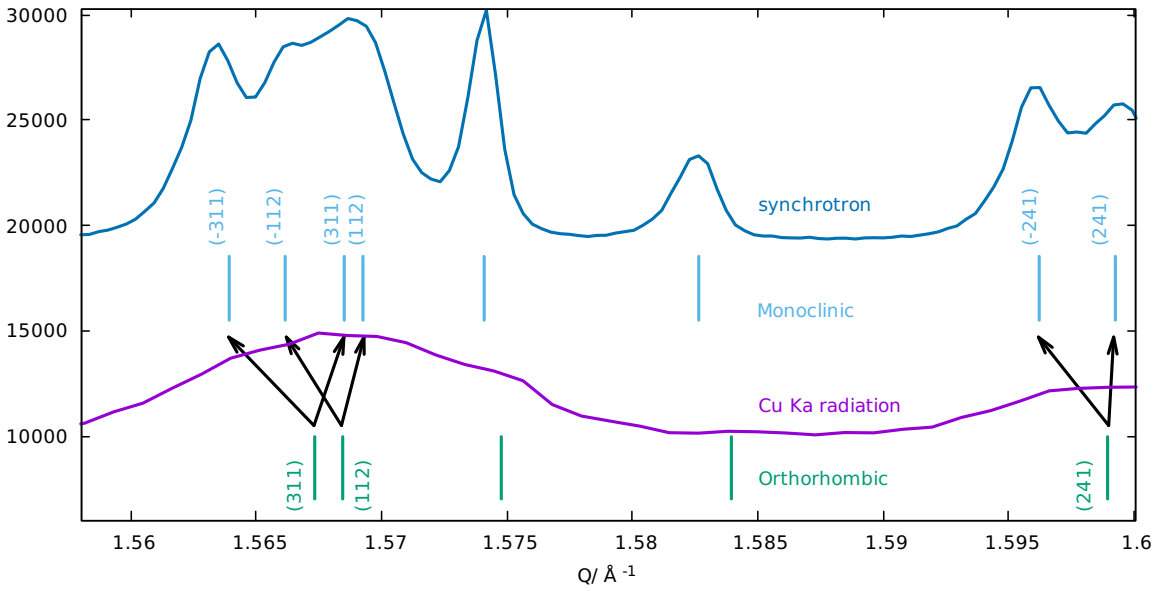

Figure S6: The orthorhombic indexing of PST–27 (green marks) fails to account for the splitting of several reflections, which is apparent in the data obtained with synchrotron radiation (purple trace) but not so obvious in the data obtained in the lab (red trace). A small monoclinic distortion (0.2°) explains the splitting (blue marks).

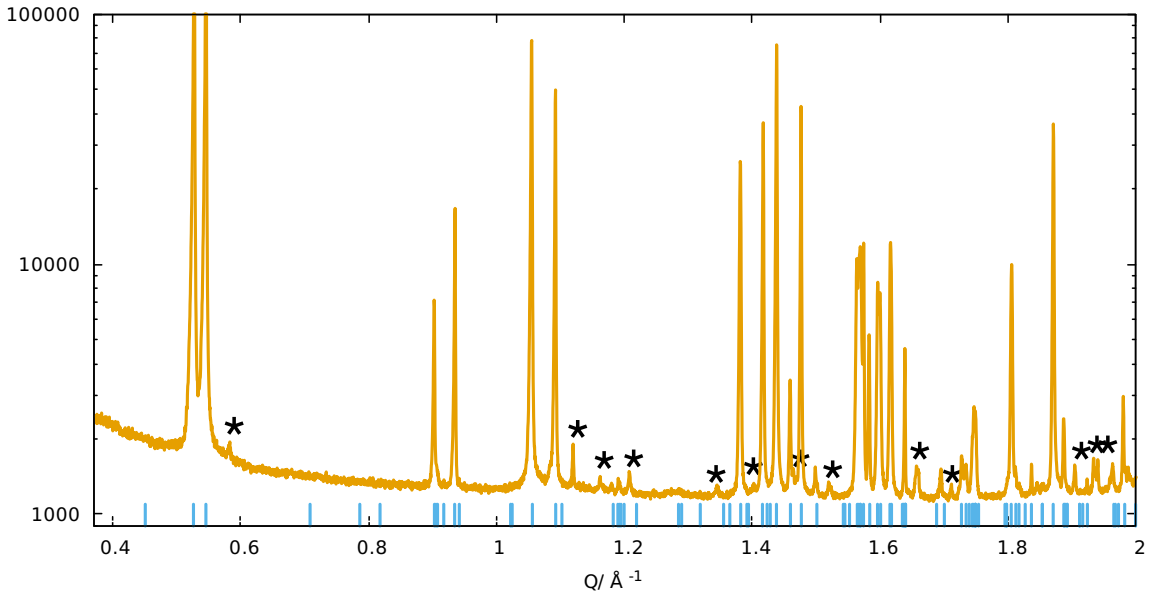

Figure S7: A number of very weak reflections (marked with *) that can not be indexed in the monoclinic *Pc* space group. Please note that the intensity scale is logarithmic to make those tiny reflections visible.

Structure analysis of triclinic $AlPO_4$–34

The structure of triclinic $AlPO_4$–34 was solved by direct methods using the Expo 2009 suite of programs.[1] Only partial solutions were found in space groups $P1$ and $P\bar{1}$ with the true chemical composition of the unit cell. However, when Al and P were substituted by Si, an essentially complete solution was obtained in space group $P\bar{1}$. In this solution, F and N were mistaken as framework O, while one O was taken as an organic N and another O as the fluoride linking two sites at the diagonals of a 4MR. These sites were at a rather close distance of 2.95 Å, and they were assigned to Al and the cited O as bridging F. The alternation of Al and P allowed to assign the whole framework T-sites. The solution contained two "organic entities" made up of C and one O that, while heavily distorted, clearly consisted of a highly planar 5 member ring with three carbons substituents on three adjacent positions of the ring, also closely coplanar to the ring, Figure S8. The cell was then reduced before Rietveld refinement.

The model obtained by direct methods in space group $P\bar{1}$ and initially with only Al, P, O and F, was used as starting model in a Rietveld refinement using GSAS,[2] and the EXPGUI graphical interface.[3] Scale factor, unit cell and profile parameters were refined, with a shifted Chebyschev function initially with 30 fixed parameters to simulate the background. Then, the atoms were allowed to move with soft restrains for distances within both tetrahedra (P-O 1.53, Al-O 1.74, O-O in PO_4 2.50, O-O in AlO_4 2.84 Å) and octahedra (Al-O 1.90, Al-F 1.90, F-F 2.29, O-O 2.78 Å). Then, the cation, without H atoms, was introduced as a rigid body and its position refined, and the atomic fractions were adjusted to account for the electrons in bonded hydrogens. The weight of the restrains was then gradually lowered and finally eliminated. Fourier techniques suggested there could be some water molecule (there are 0.3 per cell according to the chemical composition) close to the center of the 6MR. However, when the position of an oxygen placed in that position with an occupancy factor of 1/6 was refined it moved very close to one of the O in the ring. Martuccci et al. located water in morpholinium-containing SAPO-34 and CoAPSO-34 in the 8MR, instead, but they have much more water, equivalent to 1.35 H_2O per unit cell in our setting.[4] Introduction of 0.333 H_2O molecules at the inversion center (0.5,0.5,0.5) did not improve the fitting, either, so water was finally not included in the model. In the final stages, atom displacement factors (grouped by atom type; for the OSDA N1C2N3, C4C5 and C6C7C8), preferred orientation correction (Dollase method) and background (finally with 35 terms) were included in the refinement. Final crystallographic data are summarized in Table S1 and the final Rietveld plot is given in Figure S9.

Table S1: Crystallographic and Experimental Parameters for the Rietveld Refinement of as-made $AlPO_4$–34.

wavelength (Å)	0.82548
temperature (K)	293
2θ range	2.00-62.00
no. of data points	6001
no. of reflections	3186
Space Group	$P\bar{1}$
unit cell parameters (Å)	
a	9.227630(8)
b	9.28611(7)
c	9.37888(6)
α	85.2122(5)
β	77.3119(6)
γ	89.3472(6)
Cell volume (Å^3)	781.284(12)
Residuals	
R_{wp}	6.01%
R_p	4.41%
R_{F^2}	6.202%
reduced χ^2	6.822

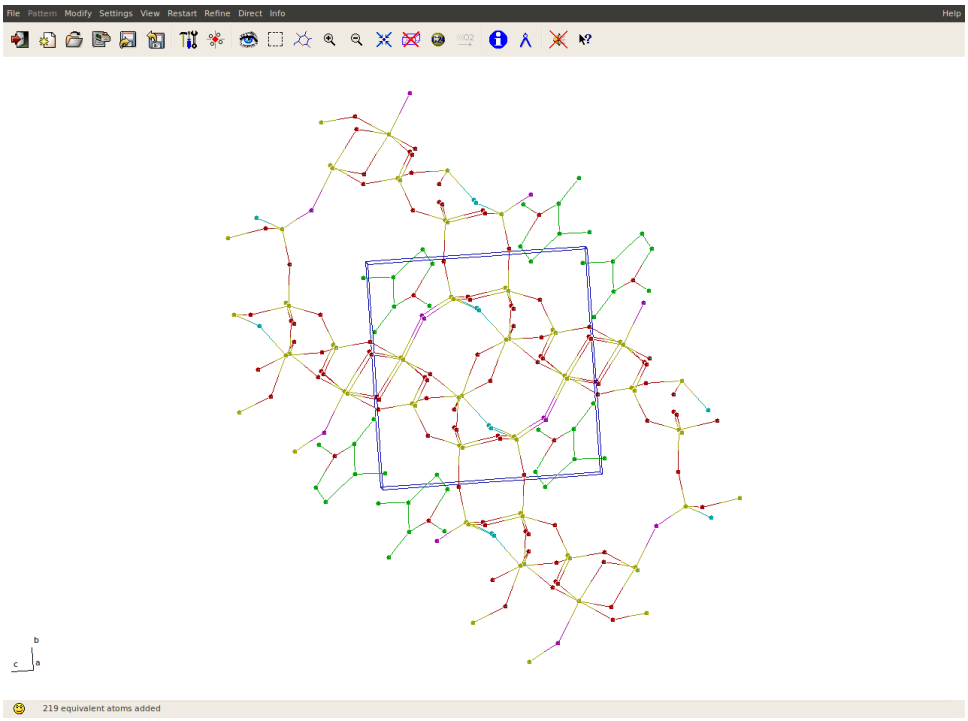

Figure S8: Solution obtained in EXPO in space group $P\bar{1}$ for as made $AlPO_4$–34.

Table S2: Fractional atomic coordinates, isotropic displacement parameters and fraccional occupancies for as-made 123TMI–$AlPO_4$–34 in space group $P\bar{1}$

atom	x	y	z	Occupancy	Uiso
Al1	0.8664(4)	0.0653(4)	0.0841(4)	1.0	0.0067(10)
P2	0.1700(4)	0.13943(32)	0.13700(32)	1.0	0.0064(4)
P3	0.3755(4)	0.12060(33)	0.67611(34)	1.0	0.0064(4)
P4	0.6209(4)	0.31593(32)	0.09528(30)	1.0	0.0064(4)
Al5	0.6232(4)	0.65829(34)	0.0856(4)	1.0	0.0076(7)
Al6	0.3956(4)	0.1193(4)	0.3395(4)	1.0	0.0076(7)
O1	0.7728(8)	0.2336(7)	0.0668(7)	1.0	0.0068(5)
F1	0.0154(6)	0.1050(5)	0.9194(5)	1.0	0.0081(15)
O2	0.5271(8)	0.0510(7)	0.6690(6)	1.0	0.0068(5)
O3	0.2540(8)	0.0126(7)	0.7460(6)	1.0	0.0068(5)
O4	-0.0001(8)	0.1447(6)	0.1855(6)	1.0	0.0068(5)
O5	0.4598(8)	0.6877(6)	0.0381(6)	1.0	0.0068(5)
O6	0.2329(8)	0.0236(6)	0.0367(6)	1.0	0.0068(5)
O7	0.3611(7)	0.1678(6)	0.5172(7)	1.0	0.0068(5)
O8	0.6493(7)	0.4751(7)	0.1242(7)	1.0	0.0068(5)
O9	0.2278(7)	0.1194(6)	0.2803(6)	1.0	0.0068(5)
O10	0.2315(8)	0.2863(6)	0.0597(6)	1.0	0.0068(5)
O11	0.3682(8)	0.2552(6)	0.7566(6)	1.0	0.0068(5)
O12	0.5117(8)	0.2546(6)	0.2333(6)	1.0	0.0068(5)
N1	0.0950(6)	0.5820(5)	0.3051(4)	1.0	0.0761(26)
C2	0.0995(5)	0.6838(4)	0.3960(4)	1.0	0.0761(26)
N3	0.2073(5)	0.6496(5)	0.4663(5)	1.0	0.0761(26)
C4	0.2737(6)	0.5213(6)	0.4183(7)	1.16667	0.174(5)
C5	0.2039(7)	0.4793(5)	0.3180(6)	1.16667	0.174(5)
C6	-0.0066(8)	0.5737(8)	0.2041(5)	1.5	0.1387(27)
C7	-0.0006(7)	0.8118(6)	0.4126(8)	1.5	0.1387(27)
C8	0.2563(7)	0.7283(8)	0.5786(6)	1.5	0.1387(27)

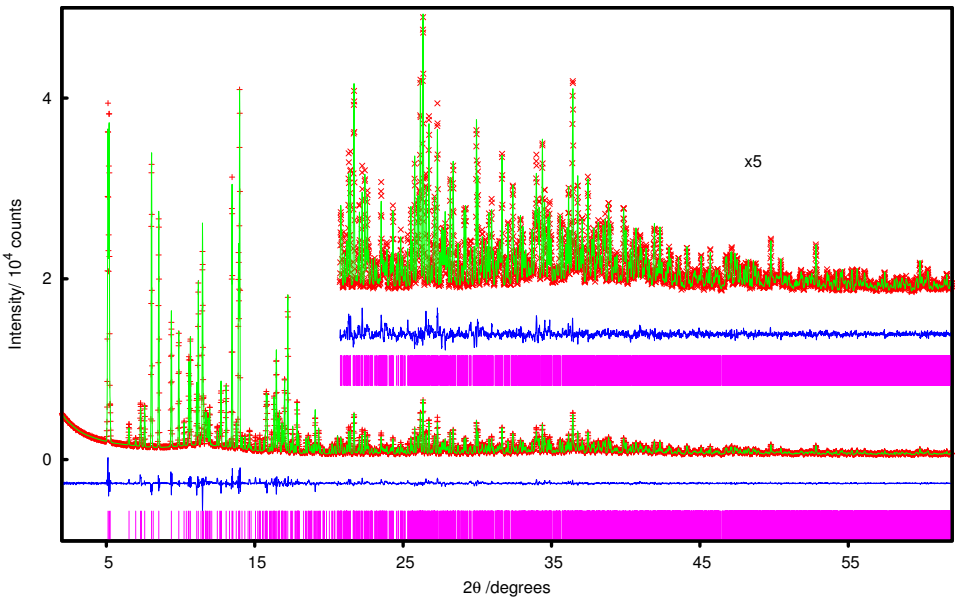

Figure S9: Observed (+) and calculated (solid line) powder X-ray diffractograms for as-made triclinic AlPO-34 ($[C_6N_2H_{11}]_2[Al_3P_3FO_{12}]_2$–CHA) refined in space group $P\bar{1}$. Vertical tic marks indicate the positions of allowed reflections. The lower trace is the difference plot. λ=0.82548 Å. .

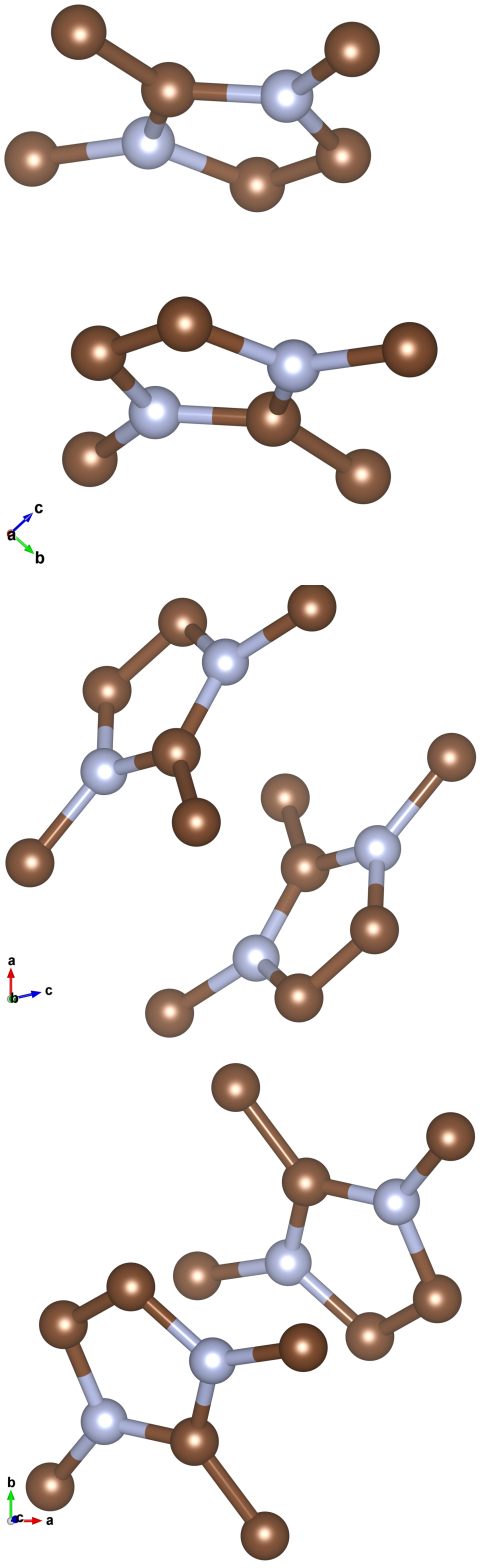

Figure S10: three views of the 123TMI$^+$ dimer

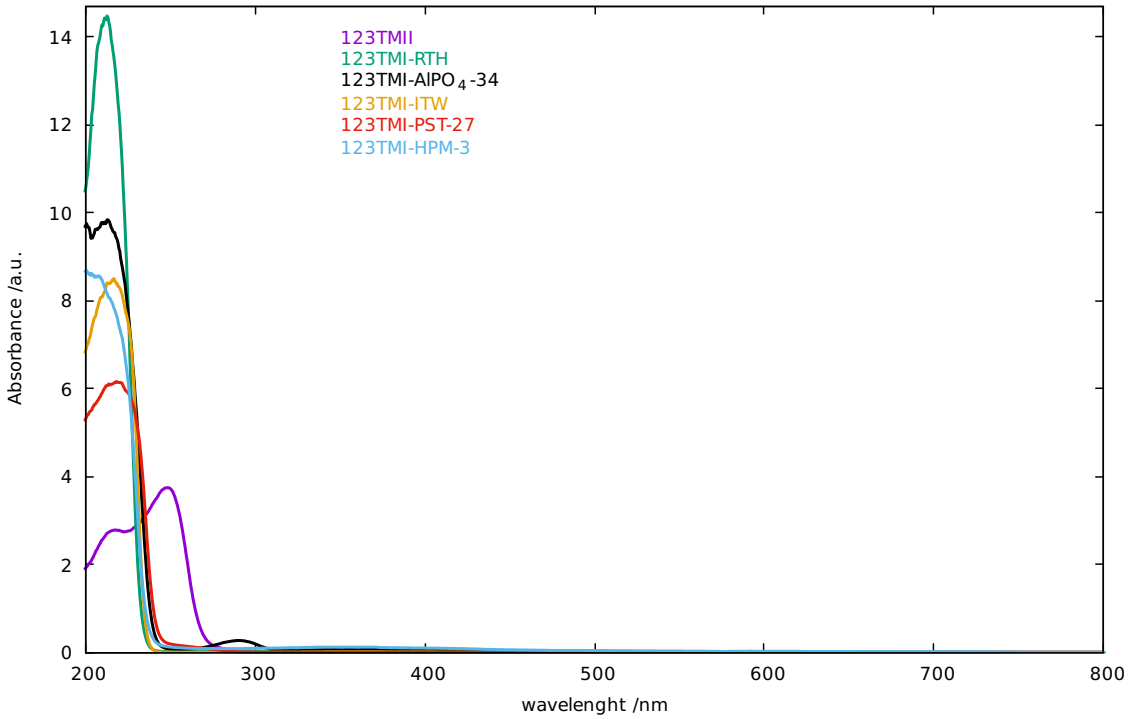

Figure S11: UVvis spectra (full range) for several 123TMI-containing solids

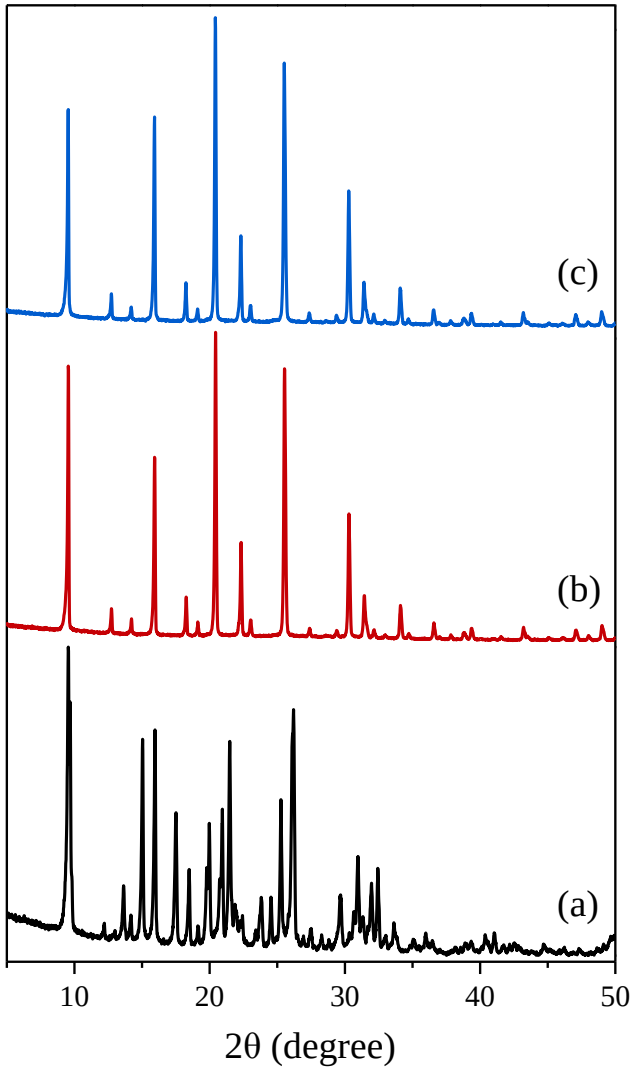

Figure S12: XRD patterns of the three SAPO–34 phases synthesized with 123TMI and F: (a) triclinic SAPO-34, (b) rhombohedral SAPO-34(1), and (c) rhombohedral SAPO-34(2)

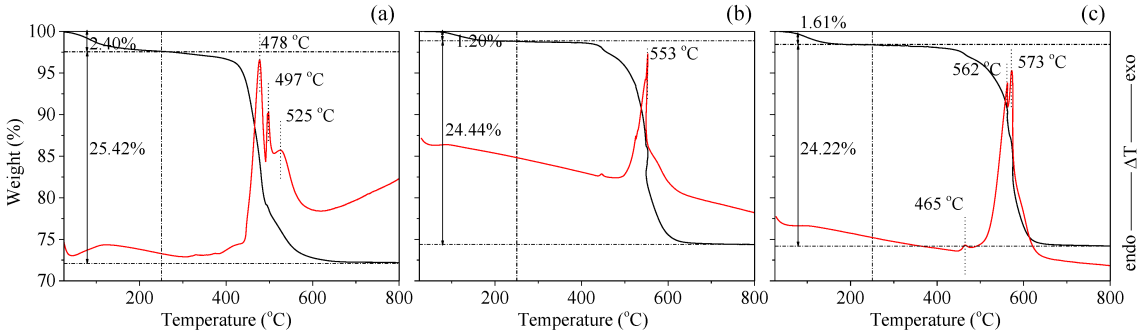

Figure S13: TGA/DTA analysis of (a) triclinic SAPO-34, (b) rhombohedral SAPO-34(1), and (c) rhombohedral SAPO-34(2).

Table S3: Chemical composition of thre SAPO–34 phases synthesized in this work

	Wt %								Unit Cell
Phase[a]	Al	P	Si	C	H	N	F	TG res.[b]	Formula[c]
t–SAPO–34	14.75	16.32	2.47	13.52	2.389	5.288	2.99	72.2 (72.8)	$(C_6N_2H_{11})_{1.95}F_{1.62}OH_{0.12}Al_{5.65}P_{5.44}Si_{0.91}O_{24}(H_2O)_{1.46}$
r–SAPO–34(1)	13.84	11.99	5.47	14.49	2.62	5.56	–[d]	74.4 (73.2)	$(C_6N_2H_{11})_{2.17}F_{1.38}Al_{5.62}P_{4.24}Si_{2.14}O_{24}(H_2O)_{2.72}$
r–SAPO–34(2)	14.25	13.78	4.52	14.99	2.45	5.89	–[d]	70.4 (72.0)	$(C_6N_2H_{11})_{2.22}F_{1.34}Al_{5.59}P_{4.71}Si_{1.70}O_{24}(H_2O)_{0.6}$

[a] t: triclinic, r: rhombohedral. [b] residue after thermal analysis, with the expected value for the formula given between parenthesis. [c] cation content determined from N content, F by analysis (t–SAPO–34, H introduced to make formula neutral) or by charge balanced (r–SAPO–34 samples 1 and 2) and H_2O from H excess. [d] not analyzed.

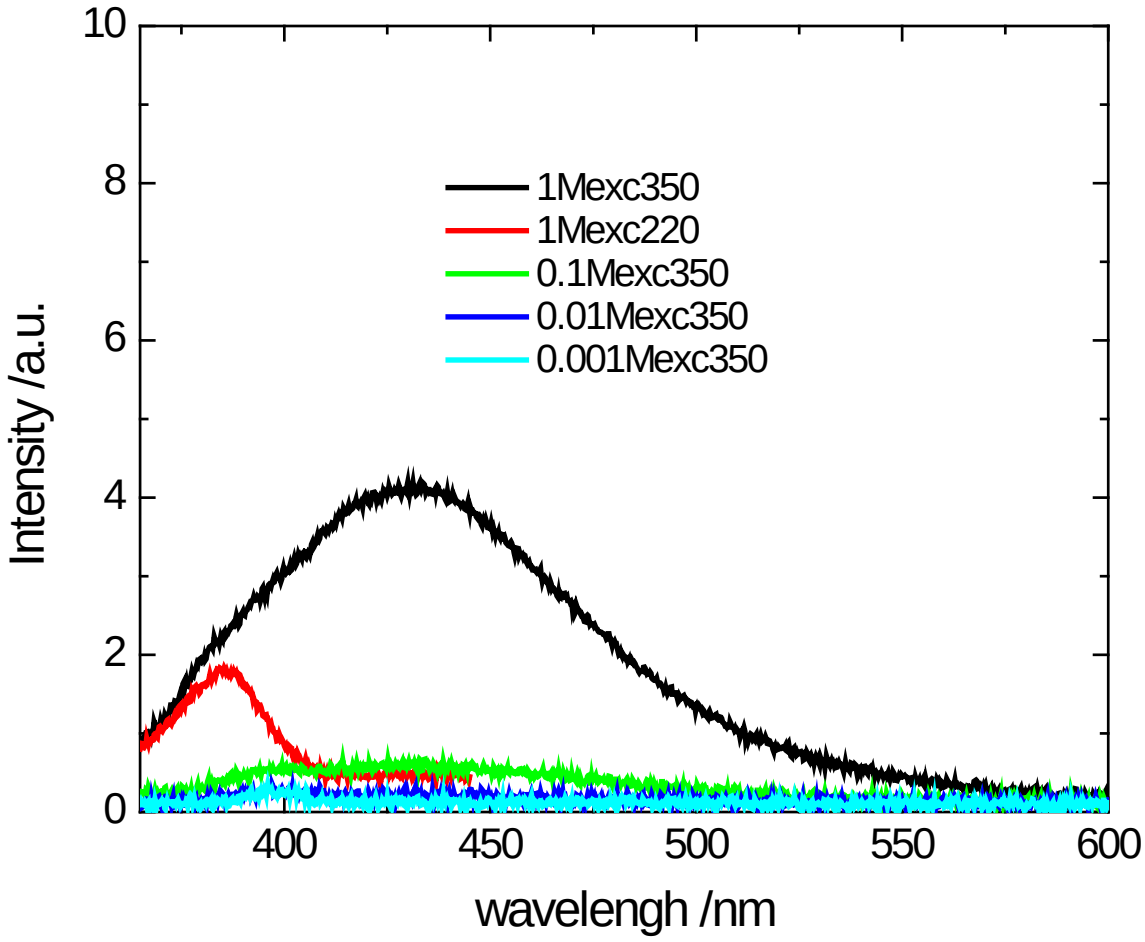

Figure S14: Emission spectra of 123TMI in water at different excitation wavelengths and/or concentrations (1 cm pathway cells, excitation and emission slits 10 and 3 nm, respectively).

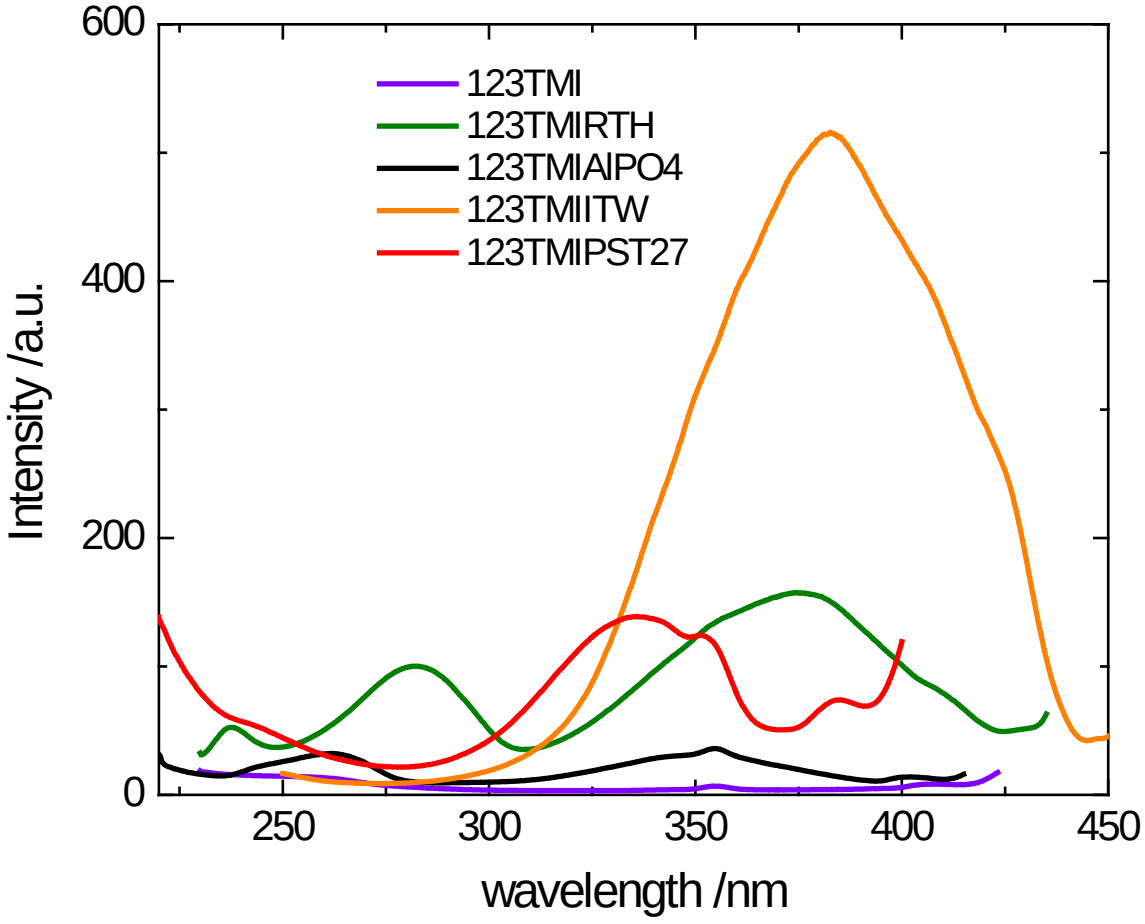

Figure S15: Excitation spectra (at the emission maximum, in the 430-460 nm range) of several solids containing 123TMI (excitation and emission slits 3 and 5 nm, respectively).

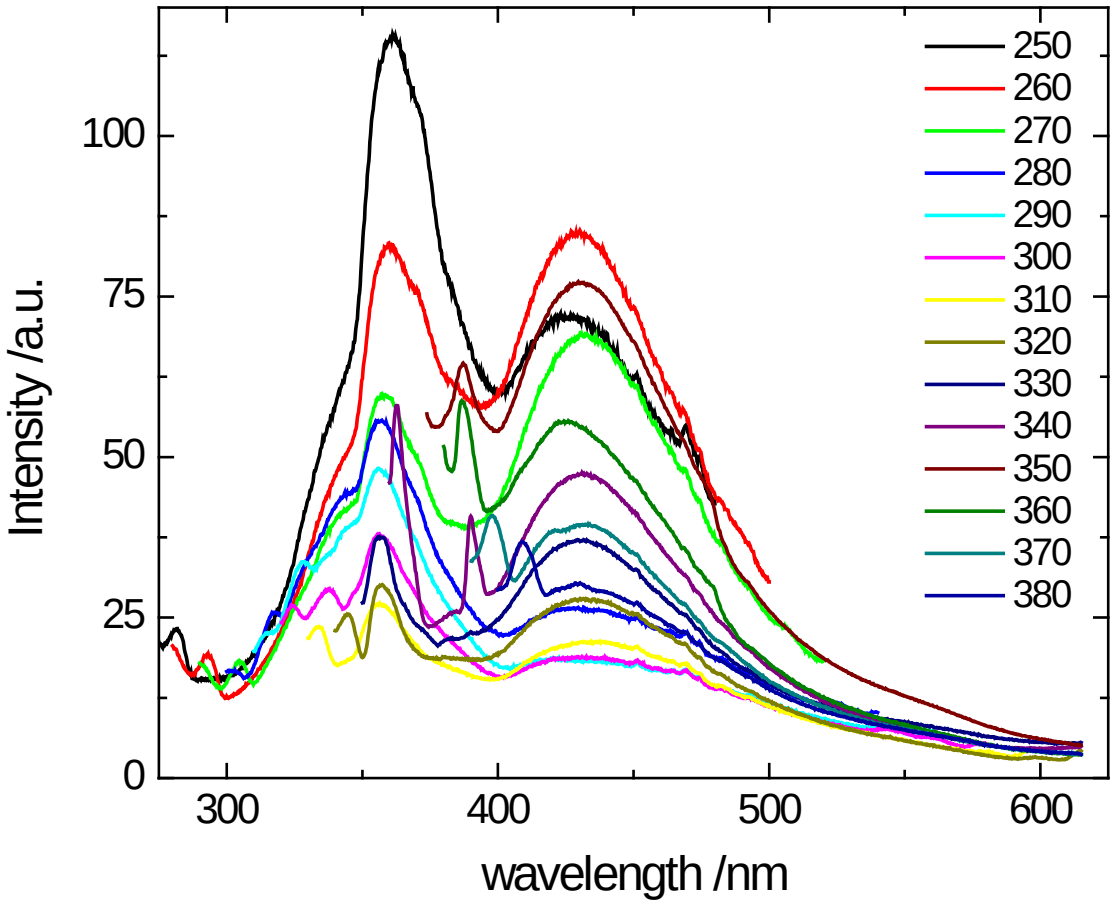

Figure S16: Emission spectra of 123TMI-AlPO4-34 as a function of the excitation wavelength (high sensibility, excitation and emission slits 3 and 1.5 nm, respectively). Sharp peaks at the beginning of every spectrum are assigned to Raman signals since they uniformly shift with the excitation wavelength.

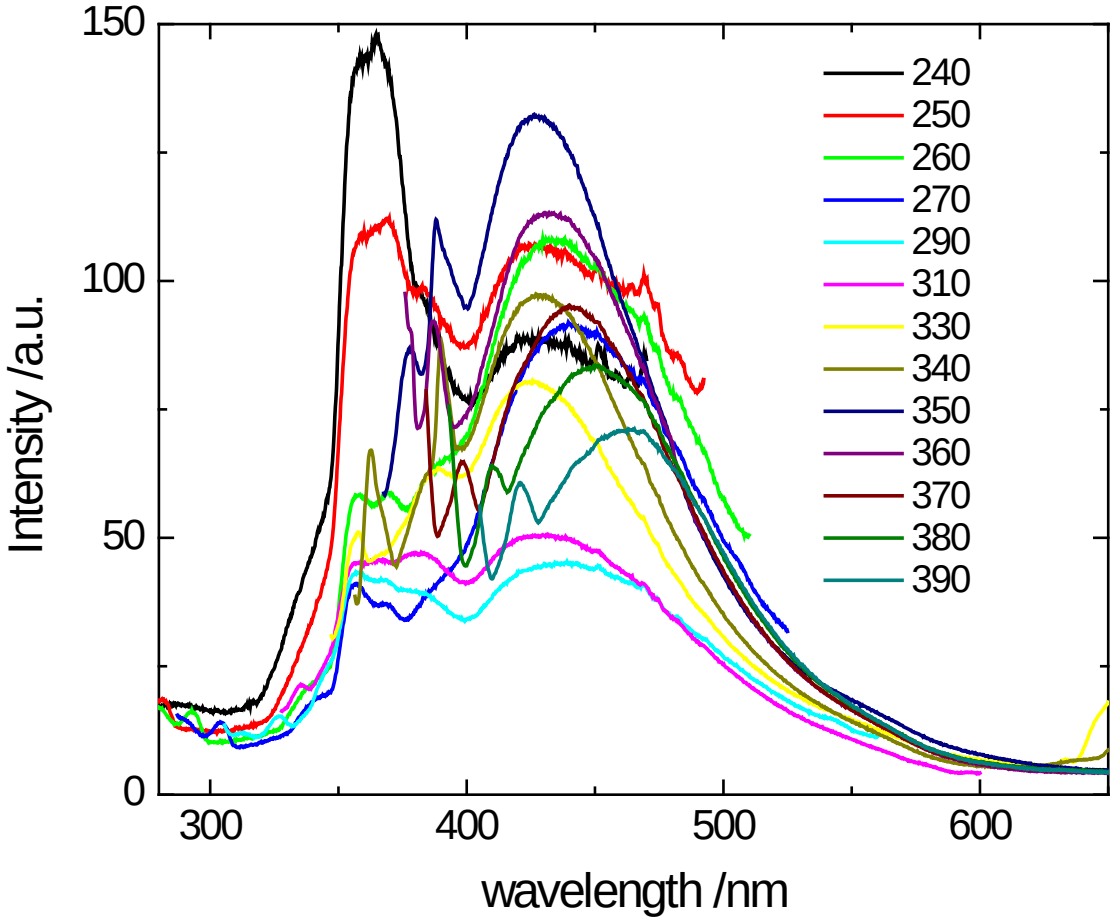

Figure S17: Emission spectra of 123TMI-SAPO-34(2) as a function of the excitation wavelength (high sensibility, excitation and emission slits 3 and 1.5 nm, respectively). Sharp peaks at the beginning of every spectrum are assigned to Raman signals since they uniformly shift with the excitation wavelength.

References

[1] A. Altomare, M. Camalli, C. Cuocci, C. Giacovazzo, A. Moliterni, and R. Rizzi, "Expo2009: structure solution by powder data in direct and reciprocal space," *J. Appl. Crystallogr.*, vol. 42, pp. 1197–1202, Dec 2009.

[2] A. Larson and R. V. Dreele, *General Structure Analysis System (GSAS).* Los Alamos National Laboratory Report LAUR 86-748, 2004.

[3] B. H. Toby, "Expgui, a graphical user interface for gsas," *J. Appl. Crystallogr.*, vol. 34, no. 2, pp. 210–213, 2001.

[4] A. Martucci, A. Alberti, G. Cruciani, A. Frache, S. Coluccia, and L. Marchese, "Combined single-crystal x-ray diffraction and ftir study of morpholiniumwater molecular complexes embedded in a chabasite network," *J. Phys. Chem. B*, vol. 107, pp. 9655–9661, Aug. 2003.